

Title Impact of cross section libraries on CASMO-4E
and CASMO-4 results
Author(s) Rantamäki, Karin; Häkkinen, Silja; Anttila, Mika
Citation Annals of Nuclear Energy
vol. 38(2011):12, pp. 2830-2835
Date 2011
URL <http://dx.doi.org/10.1016/j.anucene.2011.09.004>
Rights Copyright © (2011) Elsevier.
Reprinted from Annals of Nuclear Energy.
This article may be downloaded for personal
use only

VTT
<http://www.vtt.fi>
P.O. box 1000
FI-02044 VTT
Finland

By using VTT Digital Open Access Repository you are bound by the following Terms & Conditions.

I have read and I understand the following statement:

This document is protected by copyright and other intellectual property rights, and duplication or sale of all or part of any of this document is not permitted, except duplication for research use or educational purposes in electronic or print form. You must obtain permission for any other use. Electronic or print copies may not be offered for sale.

Impact of cross section libraries on CASMO-4E and CASMO-4 results

K.M. Rantamäki*, S. Häkkinen, M. Anttila

VTT Technical Research Centre of Finland, P.O. Box 1000, FI-02044 VTT, Finland

Abstract

A detailed comparison between the code CASMO-4 and its extended version CASMO-4E has been made. In addition to the standard library, CASMO-4E calculations have been performed also with its extended libraries. The differences are significant enough to be considered when choosing the library to be used for a particular problem. The differences in the multiplication factor k_{∞} range up to several hundred pcm depending on the void history, burnup and other parameters. The differences in fuel temperature or void coefficients are smaller especially at small void fraction and low burnup. At large void and low burnup CASMO-4E with the standard library gives significantly different results than the other combinations. The microscopic cross sections show small differences when calculated with the same library but clear differences due to the extended libraries.

Keywords: CASMO-4, CASMO-4E, cross section, multiplication factor, reactivity coefficient

PACS: 25.85.Ec, 28.20.Cz, 28.20.Fc, 28.20.Gd, 28.20.Ka, 28.41.Ak

*Corresponding author

Email address: Karin.Rantamaki@vtt.fi (K.M. Rantamäki)

1. Introduction

CASMO-4 (Rhodes and Edenius, 2004) and its extended version CASMO-4E (Rhodes et al., 2004) are widely used for calculating reactor physics constants for fuel assemblies of light-water reactors. For power companies it is essential to know the differences between these codes. Moreover, since CASMO-4E enables the use of three further libraries in addition to the standard library, it is also important to know the differences between these libraries.

The objective of this work is to enlighten the differences in various reactor physics constants due to the code versions and various libraries. The constants have been compared and are here reported for one fuel assembly type. The parameters chosen to be compared are the multiplication factor, k_{∞} , the reactivity constants and the two-group microscopic cross sections.

Section 2 describes the simulation model, the codes, libraries and parameters. Section 3 deals with the simulation results. The differences in the reactor physics constants are reported in Sec. 3.1 while the reactivity coefficients are discussed in Sec. 3.2. The microscopic cross sections of two uranium isotopes are described. Finally, a short summary is given in Sec. 4.

2. Simulation Model

In this work, the CASMO-4 (Rhodes and Edenius, 2004) version 2.05.14 and the extended code CASMO-4E (Rhodes et al., 2004) version 2.10.16P_VTT were used. CASMO-4E enables a hexagonal geometry which is important in Finland, since two of our reactors are of a VVER type. However, this option was not used in this work. The extended code CASMO-4E can also handle

Table 1: Codes and libraries used in this work

Code	Library	Source
CASMO-4	e4lblb70	ENDF/B-IV
CASMO-4E	e4lblb70	ENDF/B-IV
	e60200	ENDF/B-VI
	e60201	ENDF/B-VI
	j20200	JEFF-2.2

much more actinides and fission products than the previous one CASMO-4. A further difference between the codes is the treatment of gadolinium, Gd.

With CASMO-4, the standard library e4lblb70 based mainly on ENDF/B-IV was used (Ferri, 2001). CASMO-4E enables the use of a few other libraries. In addition to the standard library, three newer libraries (Rhodes, 2005) were chosen for this comparison study. The libraries are summarised in Table 1. In the ENDF/B-VI based library e60201 the resonance integral of U-238 has been modified so as the results to better agree with experiments (Rhodes, 2005).

The calculations presented in this paper were performed for a GE14 assembly (NEI, 2009). The bottom part of the assembly where all fuel rods are present was chosen for the study. Two cases were considered, one containing Gd as burnable absorber in 11 rods and another one without burnable absorber.

The burnup calculations were made up to 60 MWd/kgU. In the base calculation, the depletion step was 0.5 MWd/kgU until 15 MWd/kgU where the Gd is depleted. Then the step was increased to 2.5 MWd/kgU, which was

used during the rest of the calculation. All the coefficient calculations were made at burnups from 0 to 60 MWd/kgU with an interval of 10 MWd/kgU.

Two void histories were used, namely $V_h = 0\%$ and $V_h = 80\%$. The void coefficient calculations were made at intervals of $\Delta V_d = 10\%$ from $V_d = 0$ to $V_d = 100\%$. The void $V_d = 40\%$ was, however, omitted since CASMO only allows a maximum of 10 coefficient calculations.

The fuel temperature in the base case was $T_f = 900$ K. For the fuel temperature coefficient calculations the temperature was changed by $\Delta T_f = \pm 300$ K. The coolant temperature was $T_c = 600$ K throughout the calculations.

3. Simulation Results

The CASMO-4E (Rhodes et al., 2004) results were compared to the CASMO-4 (Rhodes and Edenius, 2004) results using the same standard library e4lbb70 (Ferri, 2001). The CASMO-4E results with the extended libraries e60200, e60201 and j20200 (Rhodes, 2005) were also compared to the results from CASMO-4 with the standard library. In addition to the direct comparison of multiplication factor k_∞ presented in Section 3.1, the effect of the code or library on the reactivity coefficients was also studied, see Section 3.2. Finally, a comparison of the effect on the two-group cross sections of uranium is presented in Section 3.3.

3.1. Reactor Physics Constants

The difference in the multiplication factor of CASMO-4E compared to the one obtained with CASMO-4, $\Delta k_\infty = (k_\infty^{CAE} - k_\infty^{C4}) 10^5$, is shown in Fig. 1.

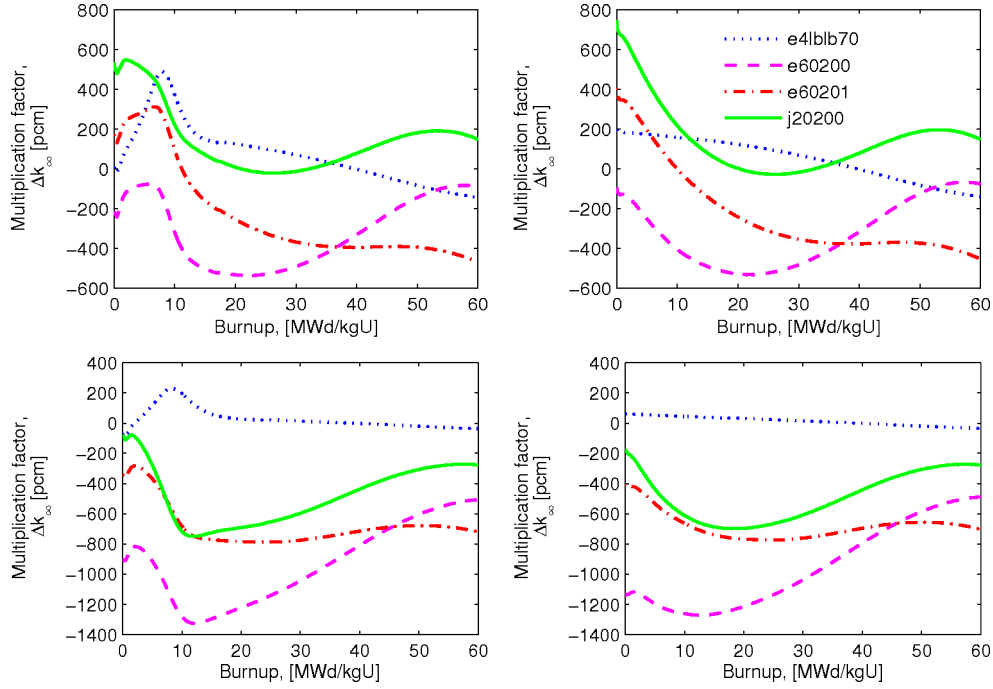


Figure 1: The difference in k_∞ of CASMO-4E compared to CASMO-4 with void history $V_h = 0\%$ on the top row and $V_h = 80\%$ on the bottom row. The left frames show the results of an assembly with Gd present and the right ones without Gd.

Here, k_∞^{CAE} refers to the multiplication factor of CASMO-4E and k_∞^{C4} to the one of CASMO-4.

In the cases with gadolinium seen in the left frames in Fig. 1, a clear bump is seen at the beginning of the lifetime. It vanishes at about 15 MWd/kgU when the Gd is depleted. After that the difference in the multiplication factor in the case with Gd follows fairly well the one without Gd. The bump in the curve is explained by the difference in the Gd treatment in CASMO-4E compared to CASMO-4. However, in both cases the differences between the codes and libraries are very large.

In the Gd calculation, CASMO-4E uses a correction method for the number densities at the end of the step (Rhodes, 2006). This method uses a sub-interval integration in which the Gd absorption rate versus number density is assumed to vary smoothly and quadratically. The method provides better accuracy for cases involving Gd where the change in k_∞ is large. However, it does not affect cases without Gd. This explains the bump seen at low burnup in the left frames of Fig. 1.

In the case of zero void history, see Fig. 1 top row, the differences range from about -500 pcm to about $+700$ pcm. Also the burnup dependences are different. After the initial bump during the Gd depletion, the difference between the two codes with the same standard library e4lbb70 decreases monotonously. The differences with the unmodified libraries e60200 and j20200 first decrease strongly and then start to rise at about 25 to 30 MWd/kgU. The difference of the modified library e60201 has a plateau at a burnup between 35 and 50 MWd/kgU.

The difference between CASMO-4E and CASMO-4 with the standard library, denoted by the dotted line in Fig. 1 is due to changes in the code version (Rhodes, 2006) in addition to the difference in the Gd treatment. The 2D transport solution in CASMO-4E uses Legendre polynomials for the polar angle integration instead of cosine-squared weighting. This results in better convergence in polar angle results. In addition, the Dancoff factor calculation is different in the two codes. CASMO-4 uses Carlvik's cylindrical collisions probabilities method where black and white boundaries, and transformation between them are used. The extended CASMO-4E code uses the method of characteristics for calculating the Dancoff factors (Rhodes, 2006). This

enables the representation of the geometry as an infinite lattice of pins in square cells. The changes explain the difference seen between the codes in the case without Gd, shown in the upper right frame in Fig. 1. In the case with Gd, in the left frame of Fig. 1, it seems that the difference in the Gd treatment compensates the difference due to the different calculation of the Dancoff factor at least at the beginning of cycle.

The difference between the two ENDF/B-VI based libraries is explained by the modification in the resonance integral of U-238 in the e60201 library. The resonance integral of U-238 has been reduced by 3.4 % (Rhodes, 2005) so that the results agree better with experiments. The energy dependence of the absorption cross section of these two libraries is shown in Fig. 2. The difference between the two libraries is clearly seen in the right-hand frame where $\Delta\sigma_{\text{abs}} = \sigma_{\text{abs}}^{\text{e60200}} - \sigma_{\text{abs}}^{\text{e60201}}$ is shown. According to the developers the unadjusted library e60200 should be used for benchmark and code comparison while the adjusted one e60201 is to be used for comparisons against experiments.

In the case of the higher void history $V_h = 80\%$, see Fig. 1 bottom row, the difference between the codes is quite small, especially when no Gd is present, i.e. in the case without Gd or when the Gd is completely depleted. However, the differences between the libraries are even larger than in the low-void-history case. At the higher void history, the differences range from -1400 pcm to $+200$ pcm. In this case, the burnup dependences increase after the initial decrease in all the extended-library cases.

Clearly, the void fraction affects the difference in the multiplication factors between the libraries. Therefore, this effect was studied using the void

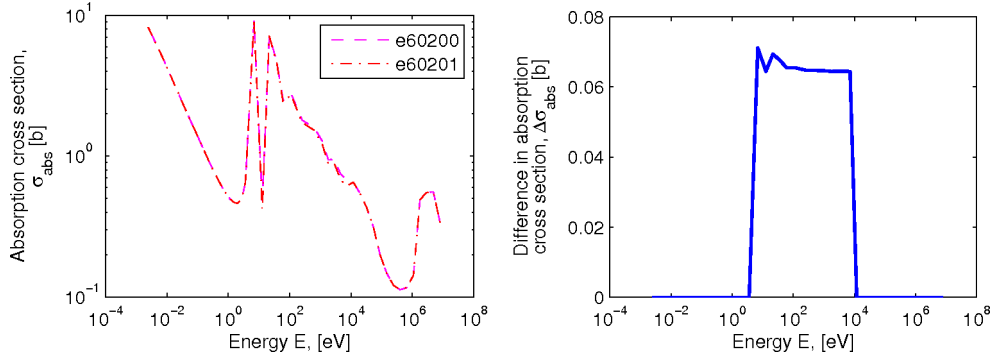


Figure 2: The energy dependence of the absorption cross section of U-238 of the ENDF/B-VI based libraries e60200 and e60201 on the left. The right-hand frame shows the difference between the two.

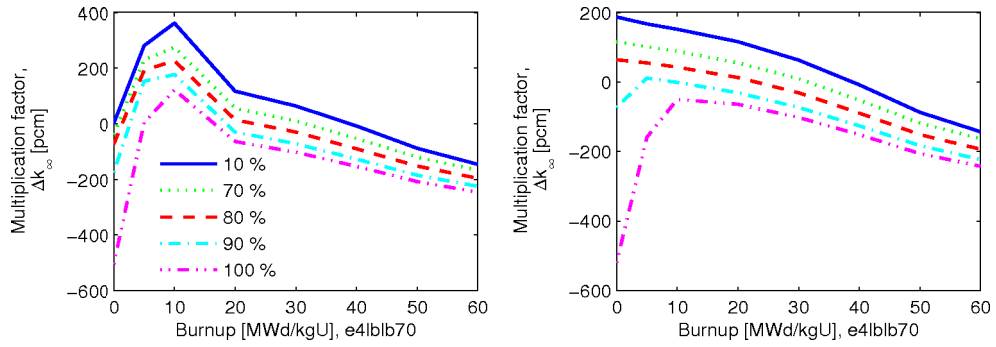


Figure 3: The difference in k_{∞} of CASMO-4E compared to CASMO-4 with void history $V_h = 0\%$ for various void fractions. The left frame shows the results of an assembly with Gd present and the right one without.

coefficient calculations and comparing the two simulations with the standard library e41b1b70. The bump at low burnup is again present at all void fractions. When Gd is present, the difference in the multiplication factor behaves in a similar way for all the void fractions. The difference is very large at low

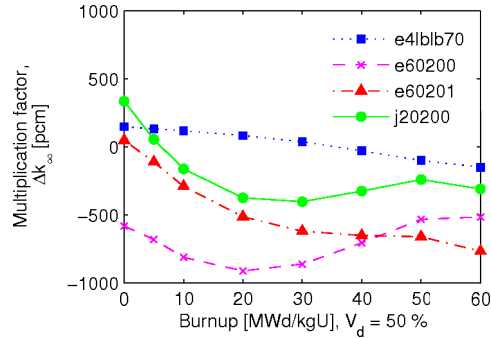


Figure 4: The difference in k_{∞} of CASMO-4E compared to CASMO-4 with void history $V_h = 0$ %, void fraction $V_d = 50$ % and no Gd for the libraries used in this work.

burnup, 0 to 10 MWd/kgU, and high void, $V_d = 90$ or 100 %, as can be seen in Fig. 3. In the case without Gd, see the right-hand side frame in Fig. 3, the different behaviour at low burnup and high void is even more distinct than in the case with the burnable absorber. At high void history, $V_h = 80$ %, the same behaviour is seen although the decrease with burnup is clearly slower than in the low-void-history case.

The comparison between the various libraries used in this work is shown in Fig. 4 for void coefficient calculation. For this example, an intermediate void fraction of $V_d = 50$ % with a zero void history was chosen. As can be seen the difference ranges from -900 pcm to $+300$ pcm, although when calculated with the standard library the difference stays within ± 150 pcm.

Unfortunately no other libraries will be introduced to CASMO-4E, so no direct comparison to any newer libraries can be made. However, in order to touch this issue, a Monte Carlo code Serpent (Leppänen, 2010) was used.

First a comparison between Serpent and CASMO-4E was done. For this

purpose the ENDF/B-VI library e60200 was chosen. The results are shown in Fig. 5 on the top row. The void is here 0 %. In the case with Gd present a clear drop in the difference of the multiplication factor is seen at low burnups. At large burnups both cases show a similar tendency of decreasing Δk_∞ with burnup. The difference in the values between the two cases, the ones with and without Gd, at large burnups is explained by the Monte Carlo method itself. In fact, in both cases the difference in the multiplication factor from Serpent with ENDF/B-VI to the one from CASMO-4 with ENDF/B-IV stays within a few hundred pcm.

Next, a comparison between newer libraries was carried out with Serpent only. The ENDF/B-VII and JEFF-3.1 based libraries were compared to the ENDF/B-VI based one. The results are shown in Fig. 5 on the bottom row. Up to half way the burnup range the results are very similar. However, after about 30 MWd/kgU the results start to deviate slightly increasing to about 200 pcm with increasing burnup. The differences in the results between the new libraries mean that the difference of these newer libraries to CASMO-4 would be quite large.

3.2. Reactivity Coefficients

Since the difference between the libraries was clear, it is interesting to see how it affects the reactivity coefficients. Therefore, the reactivity coefficients defined as $\Delta k_\infty / \Delta T_f = (k_\infty^i - k_\infty^0) / (T_f^i - T_f^0)$ was studied. Here, the superscript $i = 1, 2$ refers to the coefficient calculation at either higher or lower temperature, and the base case is denoted by the superscript 0. The void coefficients were defined in a similar way, only now the denominator at the void $(V_d^i + V_d^{i+1})/2$ was defined as $\Delta V_d = V_d^{i+1} - V_d^i$. Here, the subscript

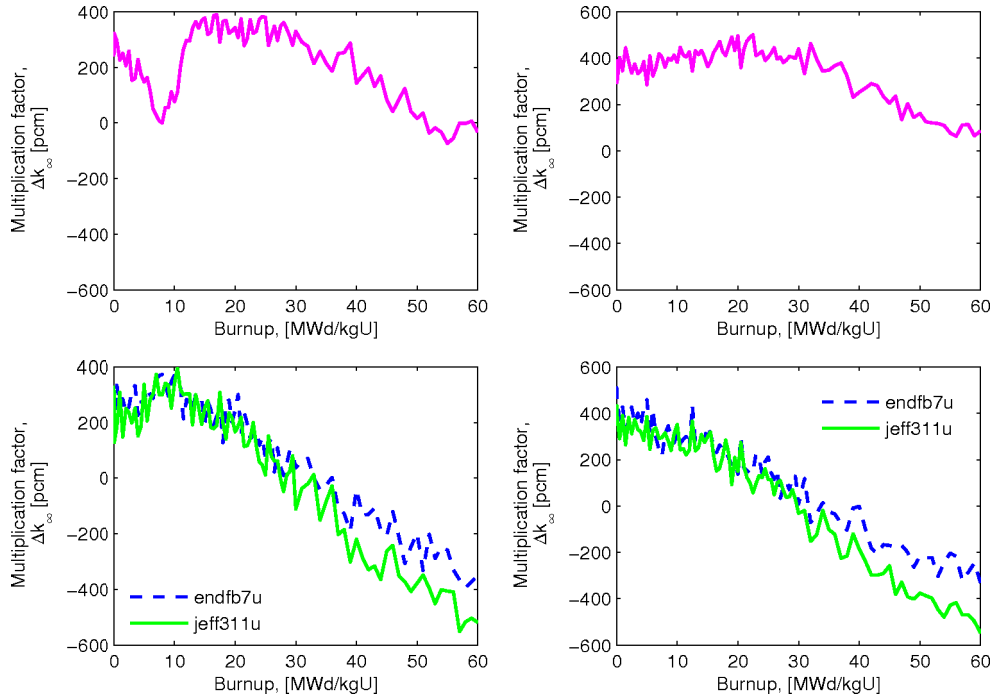


Figure 5: The difference in k_{∞} of Serpent compared to CASMO-4E for ENDF-B/VI based library on top row. The bottom row shows the difference between the denoted libraries and the ENDF-B/VI library as calculated by Serpent only. The left frames show the results of an assembly with Gd present and the right ones without Gd.

$i = 1 \dots 9$ denotes the void coefficient calculation.

The fuel temperature coefficients are shown in Fig. 6. The CASMO-4 calculation is made with the standard library e4l1b70 but denoted on the legend as CASMO-4. Clearly there are no differences between the two codes when using the standard library e4l1b70. In addition, hardly any differences are seen when comparing results calculated with the unmodified libraries e60200 and j20200 even though these results differ from those with the standard library. The modified library e60201 gives slightly larger values

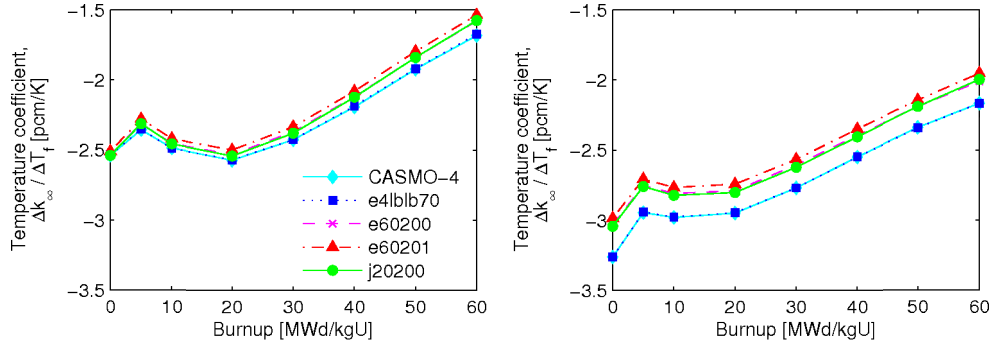


Figure 6: The fuel temperature coefficients $\Delta k_{\infty}/\Delta T_f$ at zero void and $T_f^1 = 600$ K for an assembly with Gd on the left-hand side. The right-hand side shows the same but with void history $V_h = 80$ % and an assembly without Gd.

than the unmodified libraries. The difference between the extended libraries and the standard libraries is larger at large void history, as can be seen in Fig. 6 on the right-hand side.

The void dependence of the void coefficient is shown in Fig. 7 for two burnups. Here again, the extended libraries group together and the standard-library calculations converge. Especially at higher burnup the result with the modified library e60201 deviates slightly from the unmodified ones, e60200 and j20200. A pronounced deviation of the results with the standard library from those with the extended libraries is seen at large void fraction. Where the results with the extended libraries decrease in absolute value at the end, the results with the standard library increase strongly in absolute value. A clear difference is also seen between the two codes at low burnup and high void fraction. This is consistent with the results seen in the previous section in Fig. 3 and fades with increasing burnup. Another feature seen in the data with the standard libraries is a bump in the void coefficients between

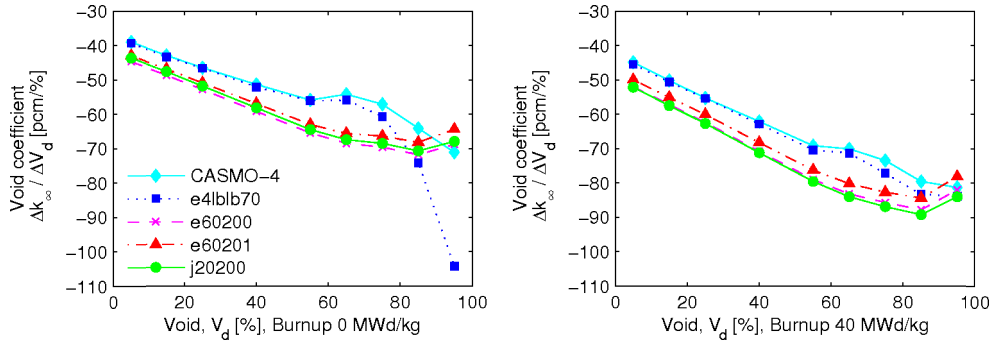


Figure 7: The void coefficients $\Delta k_{\infty}/\Delta V_d$ for an assembly with Gd at zero void history and zero burnup on the left-hand side and for a burnup of 40 MWd/kg on the right-hand side.

$V_d \approx 55\%$ and about 80% , which is seen throughout the calculations. The reason for this bump remains so far unexplained.

3.3. Two-group nuclide-specific cross sections

The standard CASMO-4/4E versions do not provide nuclide specific cross sections. They only give the nuclide specific reaction rates for absorption, fission and neutron production. However, with some modifications to the codes the two-group cross sections of those reactions can be obtained using the FRR input card.

In the case of U-235, as shown in Fig. 8, the two codes give the same results when using the standard library e4l1b70. The extended libraries deviate from these results clearly except maybe for the thermal neutron production cross section, where the results with j20200 and the standard library are overlapping. The absorption cross sections obtained with the extended libraries e60200, e60201 and j20200 are also very close. However, in the fast

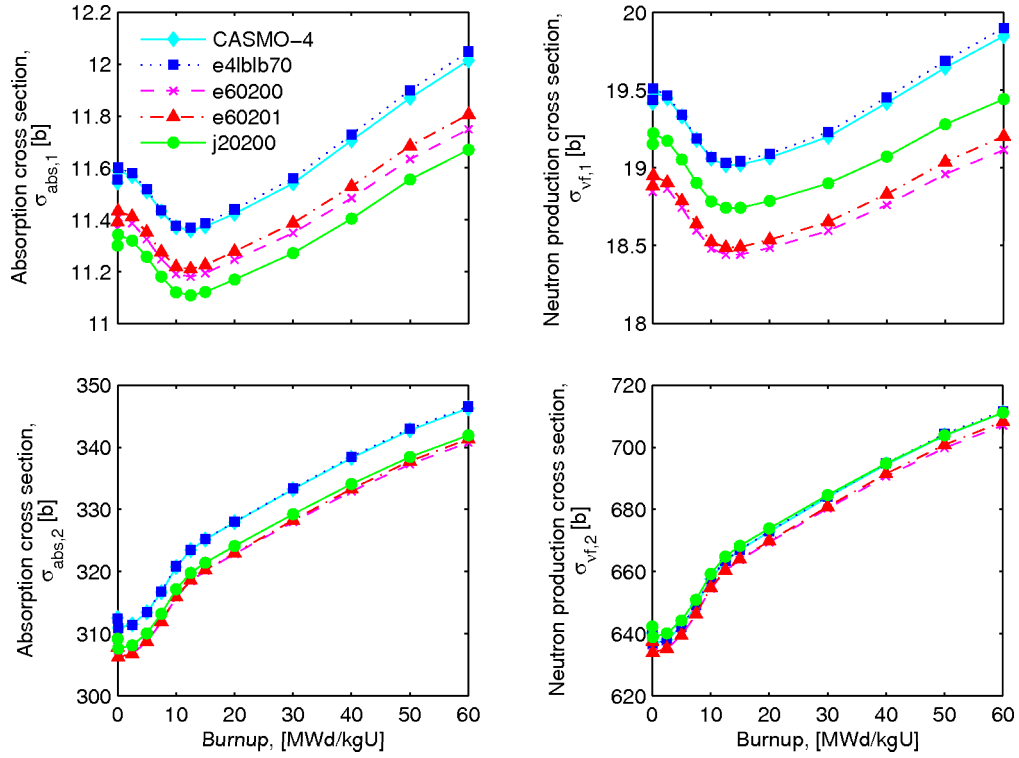


Figure 8: Two-group cross sections for U-235. On the left-hand side are the absorption cross sections and on the right-hand side the neutron production cross sections. The top row shows the cross sections of the fast neutrons and the bottom one those of the thermal group. The void history is zero and the assembly contains Gd.

group the results are different. The two ENDF/B-VI based libraries give results that are close to each other but the j20200 differs clearly. The absorption cross section is smaller than any other and the neutron production cross section falls between the two ENDF-B families. The behaviour of k_∞ is in agreement with this data since for U-235 it is the thermal group that dominates.

Since in the ENDF/B-VI library e60201 the resonance integral of U-238

has been modified, it is interesting to study the cross section of this isotope. The results of the modification can be seen clearly in the absorption cross section as now the difference between the two ENDF/B-VI based absorption cross sections in the fast group is clear. Contrary to U-235, the absorption cross section of the fast group obtained by j20200 is largest and the modified ENDF/B-VI library e60201 is the smallest. Now the CASMO-4 and the unmodified library e60200 results overlap. The difference between the largest (j20200) and smallest (e60201) absorption cross sections is about 2.5 %. In the thermal group, the absorption cross sections obtained with the standard libraries overlap as well as those with the extended libraries. However, for U-238 it is the fast group that contributes strongest.

The neutron production cross section of the thermal group for U-238 is very small. The standard library e4l1b70 does not have fission cross section so $\sigma_{\nu,f,2} = 0$ for this isotope. The cross sections obtained with the extended libraries are overlapping. In the fast group, the CASMO-4 and 4E results with the standard library are again fairly close to each other as are the ENDF/B-VI results. The results with the j20200 library are slightly smaller than the ENDF/B-VI based results. All the cross sections can be seen in Fig. 9.

4. Summary and Conclusions

The CASMO-4E results were compared to the CASMO-4 results using the standard library e4l1b70. In addition, results with the extended libraries e60200, e60201 and j20200 were compared to those with the standard library. The comparison was done on the multiplication factor, reactivity constants

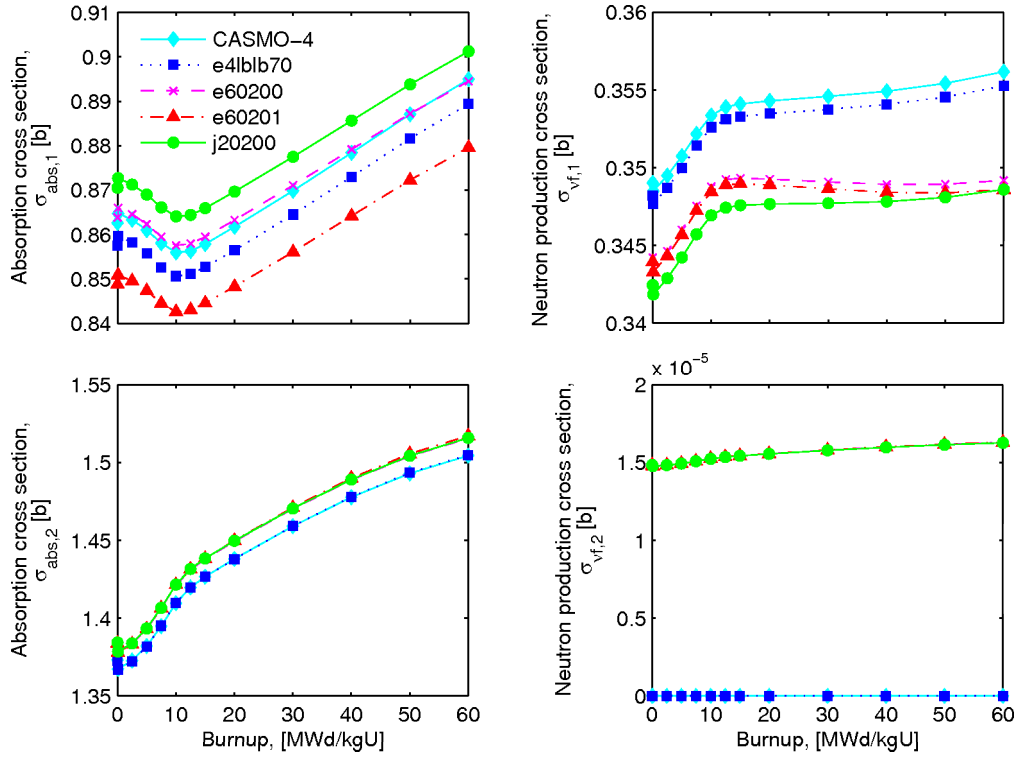


Figure 9: Same as in Fig. 8 but for U-238.

and microscopic cross sections.

The difference in the gadolinium treatment causes significant differences in the multiplication factor, k_{∞} , at low burnup, $\lesssim 15$ MWd/kgU. After the depletion of the burnable absorber, the difference in the multiplication factor calculated with different libraries is the same as for assemblies without Gd. The differences to the CASMO-4 results extend up to several hundred pcm. In general, the difference is larger at large void histories. Moreover, at low burnup the behaviour of the Δk_{∞} is different at high void fractions compared to lower void fractions.

The fuel temperature coefficients differ only slightly. The largest differences are found at large burnups and with large void histories. Also in the void fractions, the differences increase with burnup. With the standard library e4l1b70 a plateau is formed between $V_d \approx 50\%$ and 80% , which is not seen with the other libraries. Moreover, at low burnup and high void CASMO-4E with the standard library shows a significant difference in the void coefficient compared to the other libraries and CASMO-4 with the same library.

The microscopic cross sections studied in this work show small differences between the calculations with the same standard library. However, when calculated with the extended libraries clear differences are seen. These differences range up to slightly over 2% .

According to this study, there are clear differences between the two codes and also between the libraries. Even when using the same library there are differences between the codes due to e.g. Gd treatment and changes in the calculation methods. On the other hand the differences in e.g. the reactivity coefficients at low burnup and small void fractions are fairly small. Therefore there are good reasons to know and understand the differences between the libraries in order to make an appropriate choice of library for the particular problem in interest.

Acknowledgements

This work was funded through the Finnish National Research Programmes on Nuclear Power Plant Safety 2010 - 2014, SAFIR2010 and SAFIR2014.

References

- Ferri, A. A., October 2001. CASMO-4 Standard Neutron Library E4LIB Version LB Date 010417. Studsvik Scandpower, report SSP-01/462 rev 0 Edition.
- Leppänen, J., February 2010. PSG2 / Serpent - a Continuous-energy Monte Carlo Reactor Physics Burnup Calculation Code, Methodology - User's Manual - Validation Report. [Http://montecarlo.vtt.fi/](http://montecarlo.vtt.fi/).
- NEI, 2009. Fuel review: Design data. Nuclear Engineering International, 36–48.
- Rhodes, J., 2005. JEF 2.2 and ENDF/B-VI 70 Group Neutron Data Libraries. Studsvik Scandpower, report SSP-04/454 rev 2 Edition.
- Rhodes, J., 2006. Summary of CASMO-4E v2.10.xx Changes. Studsvik Scandpower, report SSP-01/460 rev 11 Edition.
- Rhodes, J., Edenius, M., 2004. CASMO-4: A Fuel Assembly Burnup Program, User's Manual. Studsvik Scandpower, report SSP-01/400 rev 4 Edition.
- Rhodes, J., Smith, K., Edenius, M., 2004. CASMO-4E: Extended Capability CASMO-4, User's Manual. Studsvik Scandpower, report SSP-01/401 rev 2 Edition.